Multiple Detection in Size-Exclusion Chromatography of Macromolecules

ARTICLE *in* ANALYTICAL CHEMISTRY · FEBRUARY 2005

Impact Factor: 5.64 · DOI: 10.1021/ac053345e

1 AUTHOR:

Andre M Striegel
National Institute of Standards and Technolo…
87 PUBLICATIONS **1,034** CITATIONS

SEE PROFILE

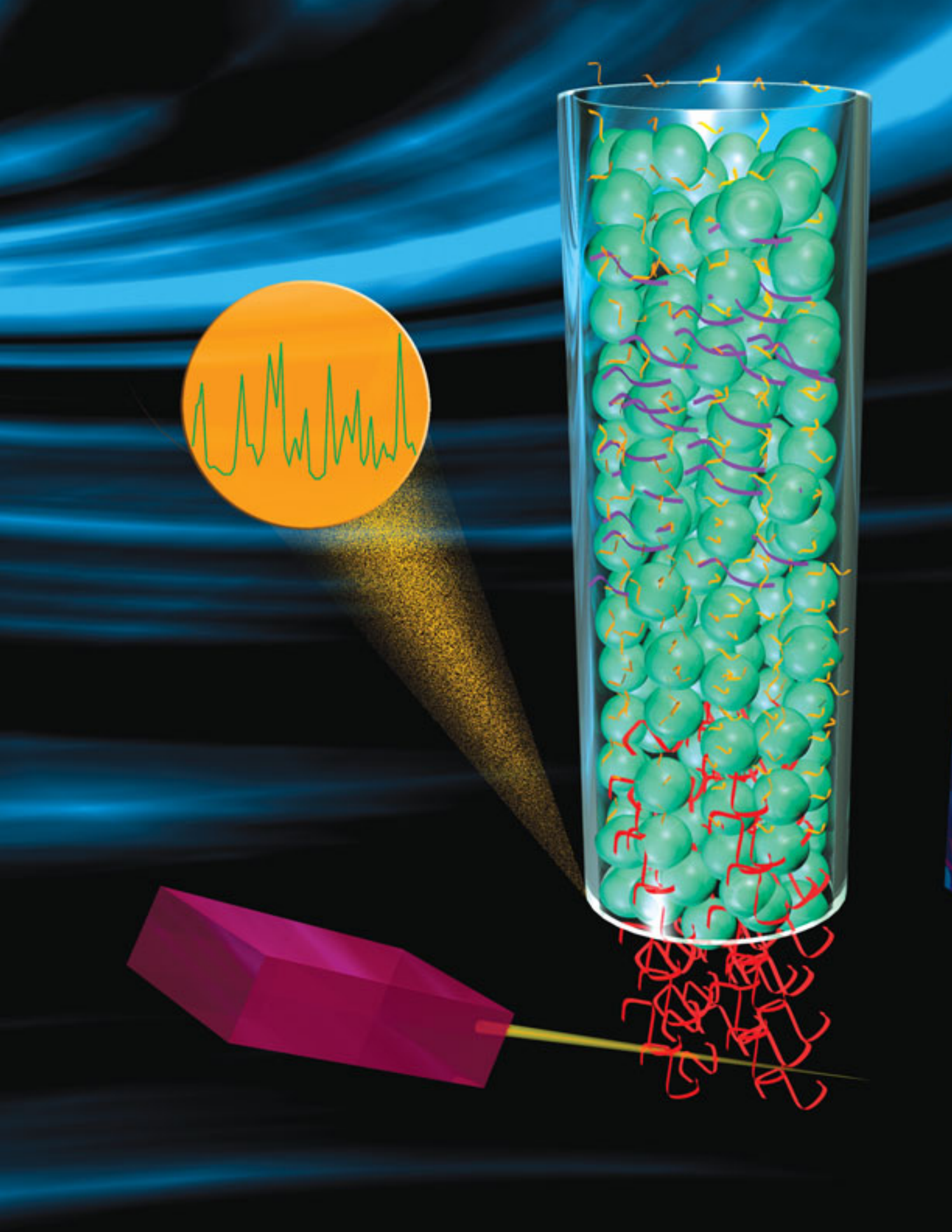

André M. Striegel
Florida State University

Multiple Detection in Size-Exclusion Chromatography of Macromolecules

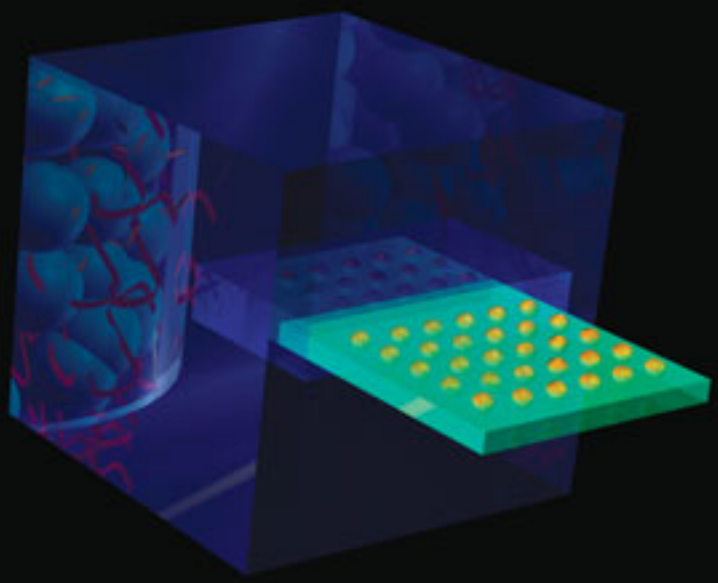

Chemical and physical detectors characterize the distributions of macromolecular parameters that have a critical effect on the end product.

Synthesizing polymers is not as exact a science as we would like it to be. Natural syntheses and even well-controlled laboratory syntheses often yield macromolecules that vary in length, molar mass, branching, chemical composition, and other properties. Characterizing these properties and their distributions is important because of their critical effect on end-use structure–property relations and, hence, on the end product itself. The most commonly studied properties are the molar mass averages (M_n, M_w, M_z, etc.) and the molar mass distribution (MMD). Various processing characteristics of macromolecules can be related to the individual averages, for example, flow properties and brittleness (related to M_n) and flex life and stiffness (related to M_z). Similarly, properties such as tensile strength and abrasion resistance tend to increase as MMD narrows, and properties such as elongation and yield strength tend to increase as MMD broadens.

During the past four decades, size-exclusion chromatography (SEC) has been established as the premier method for characterizing M averages and the distribution of natural and

synthetic polymers. Equally important, or more important, is the ability of SEC to characterize the distributions of many other macromolecular parameters (Table 1). This ability is imparted by the many analytical techniques that serve as detection methods and that are the primary subject of this article (*1*). Because of space limitations, this article will focus on SEC as the sole separation method prior to detection and ignore its growing role in 2-D LC.

Detection methods will be divided into two classes. Chemical detectors, such as UV–vis (when not used as a concentration-sensitive detector), IR, NMR, and MS, usually combine in additive fashion. Physical detectors, such as the viscometer (VISC) and light-scattering (LS) photometers, on the other hand, can combine in synergistic fashion. Some detectors appear to bridge the gap between classes; for example, IR and NMR can function as either chemical or physical detectors. The type of information provided by each class will be explored. Because of the large number of detectors covered here, it is impossible to include an explanation of the fundamentals of each. Many excellent reference sources exist on SEC, as well as on each of the individual topics (*2*, *3*); a few relevant references are given where appropriate.

SEC and the single detector

SEC operates via an inverse molecular sieving mechanism that depends on the relative size or hydrodynamic volume of a dissolved molecule with respect to the average pore size of the packing material in the column (*2*). During its passage through a size-exclusion column, a polymer molecule samples a portion of the available pore space. Certain molecules will be too big to fit into any of the pores and will elute together at the so-called total exclusion limit. Other molecules will occupy a volume so small compared with the smallest pore size that they will elute together at the total permeation limit, regardless of differences in size. Between the total exclusion and total permeation limits is the separation region of the column; here, the fraction of the sampled pore volume is inversely proportional to the size of the polymer, that is, inversely proportional to the hydrodynamic volume of the polymer. As a result, molecules occupying a larger hydrodynamic volume will elute earlier than those occupying a smaller volume. Although this behavior can correspond with larger M polymers eluting before those with smaller M, the elution order can be drastically changed by long-chain branching (LCB) and other factors.

Concentration-sensitive detectors—differential refractometer (DRI), UV–vis detector, and evaporative LS or evaporative mass detector—are by far the most widely used in SEC because they meet the minimum detection requirement for calculating M averages and distributions. Generally, the values obtained using only a concentration-sensitive detector are highly precise but of dubious accuracy. This dubiousness is caused by calibration curves that are normally constructed using narrow-polydispersity linear standards that usually do not possess the same chemistry or architecture as the analyte. Beyond their use in the construction of calibration curves, concentration-sensitive detectors are also needed for determining the distributions of M, intrinsic viscosity, and so forth, when LS and/or VISC detection methods are used. This is because the concentration of analyte in each slice eluting from the SEC column(s) is a necessary datum for calculating these parameters.

Table 1. Properties of polymers, how they affect performance, and detection modes.

Macromolecular distribution	End-use properties	Detection mode
M	Elongation, tensile strength, and adhesion	SLS
Long-chain branching	Shear strength, tack, and peel	MALS
Short-chain branching	Haze, resistance to stress cracks, and crystallinity	IR, NMR
Architecture	Flow modification, encapsulation, and diffusion	MALS/QELS/VISC (/IR, /NMR)
Chemical heterogeneity	Toughness, brittleness, and biodegradability	UV–vis, NMR, IR, MS
Copolymer sequence	Dielectric properties, miscibility, and reactivity	NMR, IR
Polyelectrolyte charge	Flocculation, binding of metals, and transport	Conductometry

Light scattering

One type of physical detector is the LS photometer, which comes in both static and dynamic varieties (*4*). In a static LS (SLS) experiment (also referred to as total-intensity LS), the light scattered from a dilute macromolecular solution is detected either at a single angle or at many angles simultaneously. At a single angle, only M information about the analyte is generally obtained, whereas at many angles, both M and size are measured. "Size" is a versatile term, because a variety of macromolecular size parameters can be measured in a multidetector SEC experiment.

When a multi-angle LS (MALS) photometer is coupled to an SEC setup that contains a concentration-sensitive detector, the amount of incident light scattered by each slice eluting from the column is measured at many angles θ simultaneously (*5*, *6*). The weight-average molar mass M_w of each slice is obtained by extrapolating the measurements at the different angles to $\theta = 0°$. Then, the M distribution of a polymer is obtained by summing over all the slices. The angular dissymmetry, or difference in the light scattered by the dilute macromolecular solution at one angle with respect to that scattered at another, is used to determine the root-mean-square radius R_g (often referred to by the misnomer "radius of gyration") of a macromolecule, defined as the root-mean-square distance of

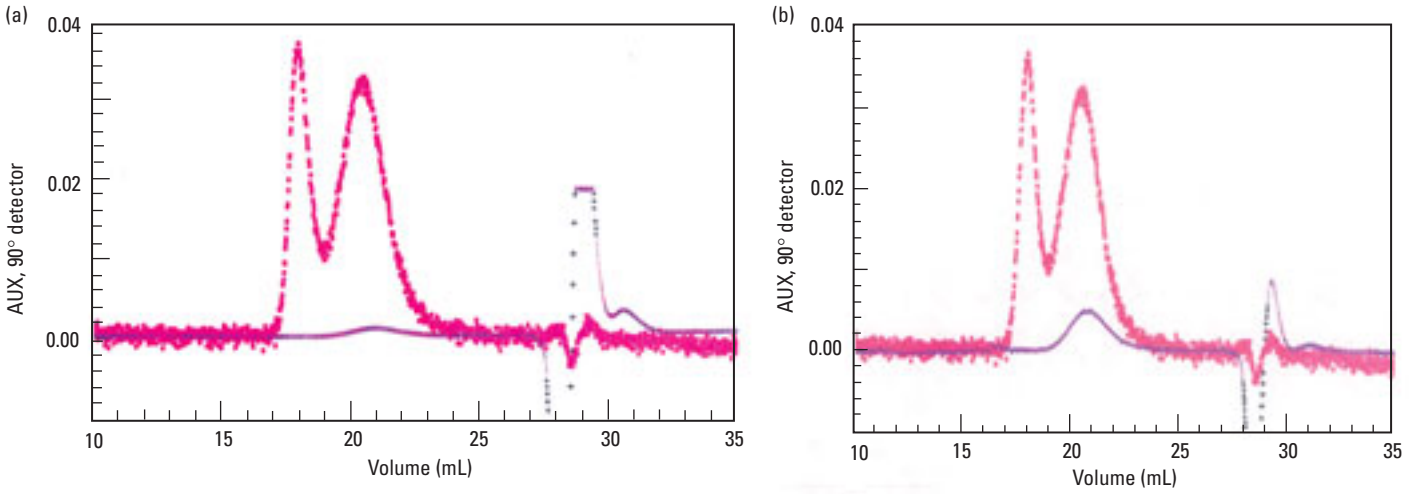

FIGURE 1. SLS sensitivity to solution aggregation of macromolecules: Pullulan dissolved in *N,N´*-dimethyl acetamide with 0.5% LiCl (DMAc/LiCl) at 80 °C.

(a) 90° SLS (pink squares) and DRI (blue crosses; AUX) signals. (b) 90° SLS (pink squares) and differential viscometer (blue crosses; AUX) signals. Unaggregated analyte elutes at ~20.5 mL, aggregated analyte at ~18 mL. No evidence of aggregation is observed by either VISC or DRI. The increase in sensitivity of SLS with increasing *M* permits even a very small concentration of a high-*M* sample, such as an aggregate, to be seen with this type of detector. (Adapted from Ref. 7.)

an array or group of atoms from their common center of mass. As a good rule of thumb, determining R_g can become difficult below ~$\lambda_0/20n_0$, in which λ_0 is the vacuum wavelength of the incident radiation and n_0 is the refractive index (RI) of the solvent, because of the lack of the necessary angular dissymmetry.

The determination of *M* averages and distributions by SEC/SLS is an absolute measurement that depends at a fundamental level only on the validity of the relationship between polarizability and RI. The accuracy of the *M* and R_g values, however, depends on the accuracy of the determination of several system parameters, such as the calibration of the SLS photometer, the normalization of the photodiodes of a MALS system, the interdetector volume(s), and the measurement of the specific RI increment $\partial n/\partial c$ of the polymer solution. This last term corresponds to the change in the RI of the solution (n) as a function of the concentration of dissolved analyte (c); this datum is necessary for accuracy in both SLS and DRI measurements. Accurate determination of $\partial n/\partial c$ (which depends on the solvent, temperature, and wavelength of the experiment in addition to the chemical identity of the analyte) can be complicated by various factors, such as copolymerization, a large oligomeric region in the MMD, and polyelectrolytic behavior.

When using SEC/MALS to study sample aggregation, researchers take advantage of the fact that the detector's response is proportional to the product of *M* and the solution concentration of the analyte. The SLS photometer is therefore referred to as an "*M*-sensitive" detector. Even a small amount of high-*M* sample will scatter a large amount of light; hence, this detector is ideal for studying the solution aggregation behavior of macromolecules. Figures 1a and 1b show the 90° SLS, DRI, and differential viscometer traces of the SEC separation of the polysaccharide pullulan (*7*). At the given experimental conditions, pullulan aggregated in solution, as evidenced by the large, early elution volume peak (retention volume ~18 mL). This aggregation was not detected by either DRI or VISC.

SEC/MALS can also be used to study LCB in macromolecules, which affects processing properties such as melt viscosity and end-use properties such as tack, peel, and shear strength (*8*; Table 1). Quantitative determination of LCB relies upon calculating g, the ratio of the mean-square radius of a branched polymer to that of its linear counterpart of the same *M*. Because the radii are measured at each slice eluting from the column, an SEC/MALS experiment can measure the LCB distribution of a polymer as a continuous function of the analyte's *M*. Figure 2a shows the so-called conformation log–log plot of R_g versus *M* for linear and branched poly(vinyl acetate) (PVAc; *9*). At any given *M*, the R_g of sample 2 (PVAc2) is smaller than that of PVAc1. This is because a molecule with LCB will adopt a more compact structure in solution than will a linear molecule of the same chemistry and *M*. Figure 2b shows the change in g as a function of *M* for PVAc2. Applying the theory developed by Zimm and Stockmayer (*10*) and assuming that PVAc2 is a trifunctional randomly branched polymer, Grcev et al. calculated the number of long-chain branches *B* and the branching frequency λ (the number of long-chain branches per 1000 repeat units of polymer) as a continuous function of *M* for PVAc2 (Figures 2c and 2d, respectively).

Note that accurate, quantitative measurement of the LCB distribution of macromolecules by SEC/MALS requires strict attention to four parameters (*8*, *10*). First, it is necessary to possess a linear standard to which the branched sample can be compared. Second, the sample and standard should have the same chemical composition. This can be complicated in the case of copolymers, in which the same chemical heterogeneity, chemical composition distribution, and so forth are also necessary. Third, the linear standard should cover the region of interest of the MMD of the branched sample. Finally, the functionality *f*, which is the number of long-chain branches emanating from each branch point, should be known a priori. Other methods exist that determine the branching distribution by comparing the intrinsic viscosities of linear and branched samples of the same *M* or by comparing the molar masses of linear and branched samples at the same elution volumes in an SEC experiment. Although useful, both these methods depend on the "draining" properties of the polymers in solution, which can lead to inaccurate results.

Self-similarity features of macromolecules, such as their fractal dimension, can also be determined using SEC/MALS (*11*, *12*). One meaning of "self-similar" is that, regardless of the length

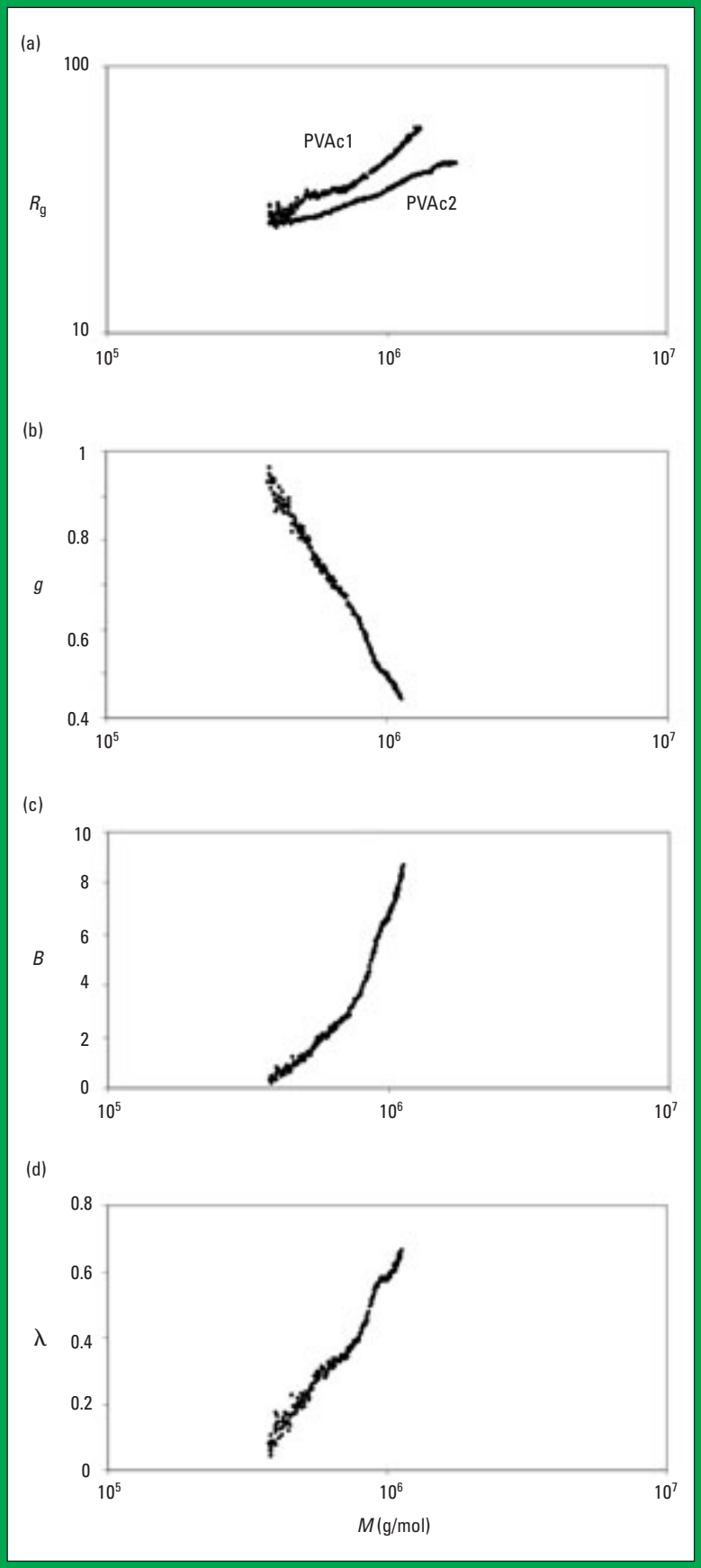

FIGURE 2. Determination of LCB distribution of PVAc by SEC/MALS.

(a) Conformation log–log plot of R_g versus M for linear (PVAc1) and branched (PVAc2) poly(vinyl acetate). (b) g, (c) B, and (d) λ as a function of M for PVAc2. (Adapted with permission from Ref. 9; figure courtesy of P. Iedema and colleagues.)

scale used to measure R_g, this parameter should scale with M in a unique fashion. A change in this scaling relationship indicates a fundamental architectural change in the polymer or a fundamental thermodynamic change in the polymer solution. The fractal dimension d_f of polymers is obtained from the conformation log–log plot of R_g versus M and is defined as the inverse of the slope α (Figure 3). The d_f of polymers can provide information that is not given by the topological dimension d_T. For example, dilute solutions of a rigid rod, a linear random coil at good solvent and temperature conditions, and a linear random coil at theta conditions (the point at which the poorness of the solvent and temperature conditions exactly compensate for the excluded volume effect) can have vastly different properties. However, these differences are not observed when the topological dimensions are compared because in all three cases $d_T = 1$. The differences are borne out, however, by d_f: $d_f = 1$ for the rigid rod, $5/3 \leq d_f < 2$ for the linear random coil at good conditions, and $d_f = 2$ for the linear random coil at theta conditions.

A specific example of this type of application is seen in Figure 3, in which the conformation plot of poly(γ-benzyl-L-glutamate) (PBLG) is overlaid upon those of two poly(vinyl butyral) samples, one with native branching (PVBN) and one with both native and induced branching (PVBX; *12*, *13*). PBLG is a fairly rigid macromolecule, as its d_f (1.20) indicates. At lower molar masses, we observed that PVBN and PVBX resemble linear random coils, with $d_f = 1.75$. At higher molar masses, d_f of PVBN is ~2, which is very close to that expected for a randomly branched polymer at good solvent and temperature conditions ($2 \leq d_f < 2.28$ for the generic case). The relatively high $d_f \approx 2.4$ of the branched region of PVBX indicates the heterogeneity of branching in this polymer, which contains both native and induced branching and may also include branch-on-branch-type structures.

A variation on SLS is the low-angle LS (LALS) photometer. Long used as an SEC detector by many researchers in the 1970s and 1980s, it fell out of favor when multi-angle systems were introduced and became popular. A new low-angle instrument with a redesigned optical arrangement was recently introduced for on-line SEC measurements, as part of a triple-detector array combining LS, VISC, and DRI (*14*). In an SEC/LALS experiment with $\theta \leq 7°$, M_w of each slice was determined without extrapolating to an angle of 0°. Although this experiment can determine a polymer's M with extreme accuracy, no size information by way of R_g is obtained because angular dissymmetry cannot be measured using a single angle.

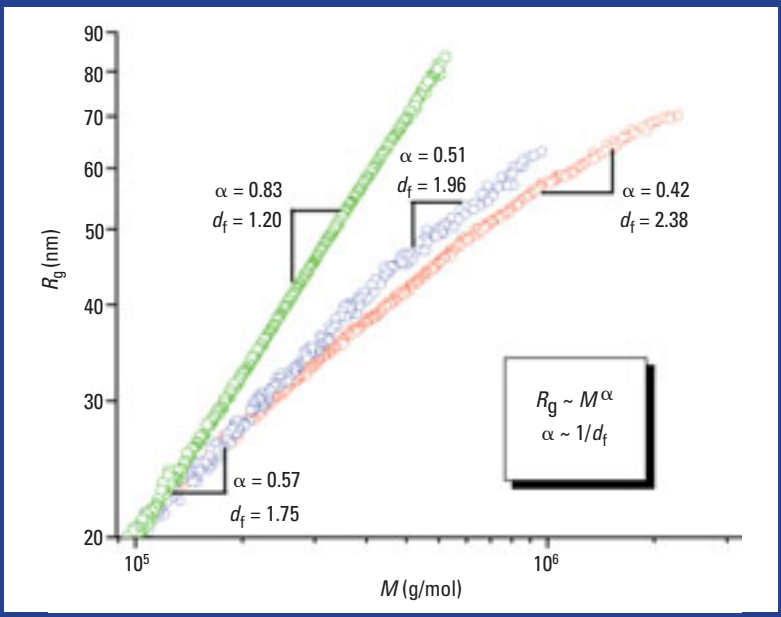

FIGURE 3. SEC/MALS provides d_f.

Conformation plots of poly(γ-benzyl-L-glutamate) (PBLG; green) and poly(vinyl butyral) with native branching (PVBN; blue) and with both native and induced branching (PVBX; red). (Adapted from Ref. 13.)

MALS detectors can also be decoupled from the SEC system for off-line use in what are called batch-mode experiments (*4–6*, *12*). These experiments can provide information that directly complements that obtained by on-line SEC/MALS studies. The basic experiment consists of measuring the scattering at many angles for a series of solutions at different concentrations. The results for each concentration at each angle are plotted. The angular data are then extrapolated to a concentration of 0, and the slope of the extrapolated line gives R_g. The concentration data are extrapolated to an angle of 0°, and the slope of this extrapolated line gives A_2, the second virial coefficient, a fundamental property of polymer solutions that is correlated with solubility, solvation, and conformation. From the common y intercept of the two extrapolated lines, M_w is obtained. Figure 4 is an example of a plot that results from this dual-extrapolation procedure (also called a Berry plot) for the PVBX sample described earlier. The results from a batch-mode MALS experiment can be used to calculate another size parameter, the thermodynamic radius R_T, which can be thought of as the radius of a sphere with the same excluded volume as the polymer (*11*, *15*).

In a dilute solution or suspension, the consequence of the dissolved particles continuously colliding with solvent molecules is random thermal (Brownian) motion, which causes the intensity of scattered light reaching a photodiode to fluctuate with time around some average value. In SLS, the time-averaged fluctuations of the scattered light are measured, whereas in quasi-elastic LS (QELS; also referred to as dynamic LS and photon correlation spectroscopy), it is the time-dependent fluctuations that are of interest (*4*, *16*). Through QELS, we obtain our third size parameter, the hydrodynamic or Stokes radius R_h, which may be thought of as the radius of an equivalent hard sphere that would feel the same force due to flow as would a macromolecule (*11*, *15*). Determination of R_h down to a few nanometers is possible with QELS.

In several modern instruments, SLS and QELS are housed in a single apparatus, obviating the need to determine interdetector volumes between the two systems. Recently, Liu et al. used SEC with both dual-angle SLS and QELS to determine the M, size, and conformation of several synthetic polymers (*17*). They used relations derived by Burchard (*11*) to combine R_g and R_h into a single dimensionless parameter $\rho \equiv R_g/R_h$ and obtain information about conformation and dilute solution thermodynamics across the MMD of poly(dimethyl siloxane). More recently, Cotts combined the capabilities of MALS, QELS, VISC, and SEC to provide architectural information, as a continuous function of M, for structures ranging from semi-rigid rods to random coils to stars (*18*).

Viscometry

The pressure drop ΔP across a capillary is related by Poiseuille's law to the length L and radius r of the tube and to the viscosity η of the solution flowing through the capillary at a volumetric flow rate Q by

$$\Delta P = \frac{8L\eta Q}{\pi r^4}$$

This equation constitutes the operating principle of single-capillary viscometers. Although it has been used for studying many natural and synthetic polymers, the differential viscometer is becoming more popular. The differential viscometer is usually a fluid-flow analog of the classic Wheatstone-bridge electrical circuit (*19*). A differential pressure transducer measures the change in pressure across the bridge, and an inlet pressure transducer measures the pressure change through the bridge. The differential pressure transducer signal is proportional to the specific viscosity η_{sp} defined by

$$\eta_{sp} = \eta_{rel} - 1 = \frac{\eta - \eta_s}{\eta_s}$$

in which η is the viscosity of the polymer solution, η_s is the viscosity of the neat solvent, and η_{rel} is the relative viscosity of the solution ($\eta_{rel} \equiv \eta/\eta_s$).

Of primary interest when using VISC with SEC is the determination of the intrinsic viscosity, $[\eta]$, and how it changes with M. The definition of $[\eta]$ is

$$[\eta] \equiv \lim_{c \to 0} \frac{\eta_{sp}}{c}$$

in which $[\eta]$ is recognized as the ratio of the signal from the viscometer (which measures η_{sp}) to the signal from the concentration-sensitive detector (which measures c) for the same data slice, after correction for interdetector delay. The units of $[\eta]$ are deciliters per gram, so intrinsic viscosity may be thought of as inverse density. The measurement of $[\eta]$ may be combined with that of M to define the

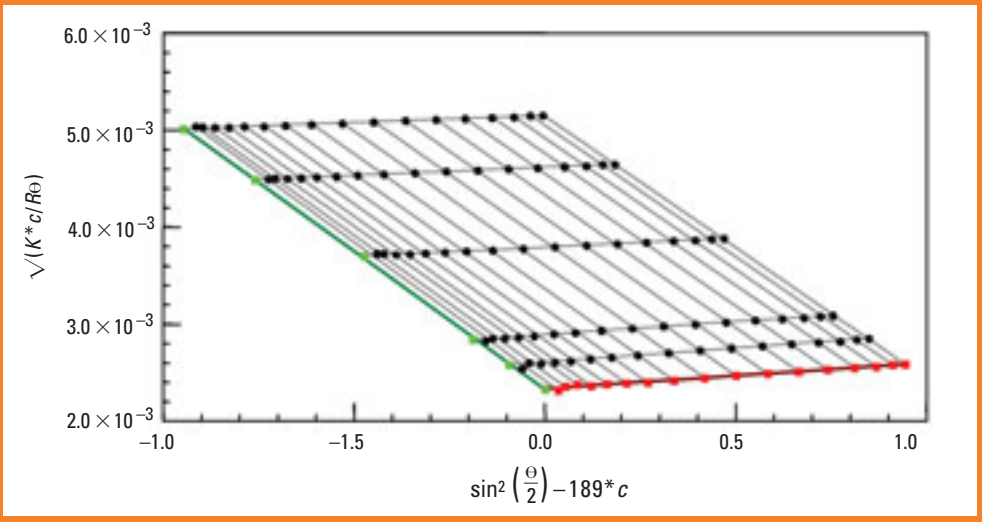

FIGURE 4. Berry plot of PVBX from off-line, batch-mode MALS data; M_w, R_g, and A_2 were determined from scattering measurements taken simultaneously at 17 different angles from a series of dilutions of PVBX.

fourth size parameter, the viscometric radius R_η of a macromolecule (*11*).

R_η can be thought of as the radius of a solid sphere that can dissipate (as heat) the same amount of the flowing solvent's kinetic energy as does the polymer, or as the radius of a solid sphere that increases the fluid's viscosity by the same amount as does the polymer (*15*). As with R_h, determining R_η into the single-digit nanometer range is possible; thus, we see that SEC/VISC and SEC/QELS can measure macromolecular size with a high degree of accuracy and precision to a much lower limit than SEC/MALS can. Naturally, the "size" that is measured by each technique is different.

Accurate information on polymer draining is needed for the quantitative calculation of the LCB distribution. Because the Mark–Houwink plot of log [η] versus log M is normally less noisy than the conformation log–log plot of R_g versus M, SEC/VISC is generally a more sensitive method than SEC/MALS for determining the presence of LCB (*8*). Figure 5 is an example of a Mark–Houwink plot used to detect LCB in two polyethylene (PE) samples, one linear and one branched (*20*). Because LCB tends to manifest more markedly in polymers with increasing M, the slope of the Mark–Houwink plot of the branched PE decreases with increasing M, whereas the slope of the linear PE remains constant as a function of M. The d_f can also be calculated from SEC/VISC data using the relation $d_f = 3/(1 + a)$, in which a is the slope of the Mark–Houwink plot (*8*, *11*). This is a useful definition, although it should be approached with caution because of potential polymer draining and coil interpenetration effects.

The four main size parameters are the R_g, R_h, R_η, and R_T radii. The first three, along with their distributions, can be measured as continuous functions of M in a single SEC/MALS/QELS/VISC experiment using commercially available detectors; R_T is obtained through off-line, batch-mode MALS. Burchard has done extensive work on the relationship of ρ to polymeric architecture and dilute solution thermodynamics (*11*). For example, for a monodisperse, linear random coil, ρ = 1.504 at theta conditions and 1.78 at good solvent and temperature conditions; for a tetrafunctional star at theta conditions, ρ = 1.33 when the arms are of uniform length but 1.534 when the arm length is polydisperse. Other ratios of the four radii have not been explored as extensively as ρ; the majority of the work has been devoted to star polymers (*11*, *21*, *22*).

The molecular radii have also been used to define the polymer draining function ($\Phi \propto R_\eta/R_g$) and the coil interpenetration function ($\Psi^* \propto R_T/R_g$); Φ describes the penetration of the hydrodynamic volume of the polymer by a solvent molecule, and Ψ* describes the interpenetration of the hydrodynamic volumes of two connected polymer segments. Though both functions have been combined in $V_{A2\eta}$ ($\propto R_T/R_\eta$), its usefulness, along with that of the polymer draining and coil interpenetration functions, has thus far been restricted to star polymers (*11*, *12*). SEC/MALS/QELS/VISC could be used to explore the dependence of ρ, Φ, and other ratios—along with the thermodynamic and architectural information these provide—as continuous functions of M for polydisperse macromolecules, but this potential remains largely untapped.

We will next discuss interfacing SEC to chemical detectors. As in earlier sections, we will deal only with on-line detection methods or with techniques used in continuous off-line mode. The

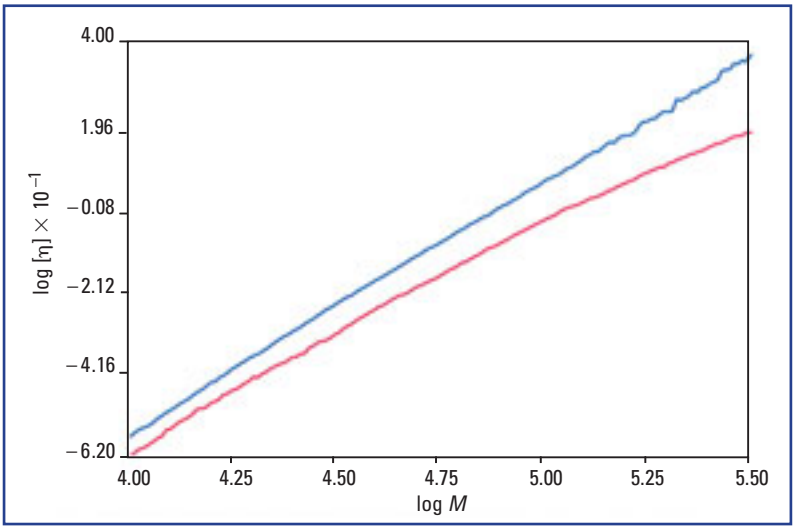

FIGURE 5. Mark–Houwink plot of linear (blue) and branched (red) PEs obtained by SEC/VISC using a differential viscometer and universal calibration. The slope of the linear PE remains invariant as a function of M, and the slope of the branched PE decreases as M increases, in the presence of LCB.

widely used practice of collecting a few discrete fractions of eluate for subsequent analysis is not discussed, because it does not provide a continuous distribution of the measured parameter.

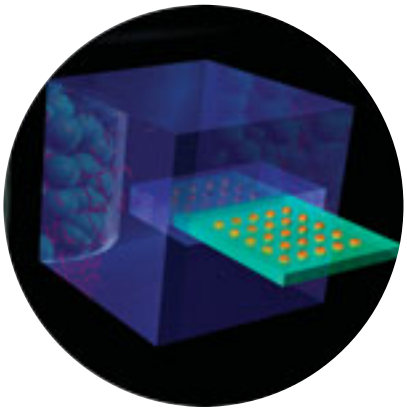

Some detectors appear to bridge the gap between classes; for example, IR and NMR can function as either chemical or physical detectors.

MS detection

ESI is the softest ionization method currently available in MS. Soft ionization combined with ESI's inherent multiple charging mechanism have made MS an ideal tool for studying biopolymers and for accurately determining their molar masses. Beyond its application to perfectly monodisperse analytes, ESI-MS has also been used in a variety of other polymer applications (*23*). As an on-line detection method, ESI-MS has been used to obtain more accurate SEC calibrations than those obtained via traditional approaches, to obtain chemical composition distribution information on copolymers, and to study humic and fulvic acids. Because only ~1% of the SEC effluent is needed for ESI-MS, other detectors are usually used. Because of their low microliters-per-minute flow rates, micro-SEC columns can be utilized. Deery et al. used SEC/ESI-MS to study 5000-Da and 12,000-Da dextrans and enzymatically digested arabinoxylan polysaccharides (*24*). They also used SEC/ESI-MS^n to determine glycosidic linkage of permethylated arabinogalactan oligomers.

In contrast to ESI-MS, multiple charging is not usually observed in MALDI MS; therefore, interpretation of the MALDI information and its use in calculating *M* are more straightforward than in ESI-MS. Fei and Murray combined SEC on-line with aerosol MALDI for the complete mass spectra, across the entire elution profile, of 1000-Da poly(ethylene glycol) and poly(propylene glycol) (*25*).

A more popular approach is continuous off-line MALDI. Using a homemade apparatus, Lou and van Dongen electrosprayed the SEC eluent and a coaxially added matrix material onto a MALDI plate (*26*). Others have used a commercially available interface in which the SEC eluent in sprayed directly through a heated capillary nozzle onto a moving MALDI target precoated with an appropriate matrix. For polydisperse macromolecules, a continuous track of sample is deposited onto the matrix surface of the target; spectra are obtained from different positions on the track. Esser et al. used this approach to study polystyrene 32500 and poly(methyl methacrylate) (PMMA) 10900 to obtain both *M* and copolymer composition of a diblock copolymer of *n*-butyl methacrylate and PMMA (*27*).

Matrix selection is an important challenge, and currently only a few different types of matrix materials have been coated onto commercially available targets. Recently, Liu et al. used poly(dimethyl siloxane)s to compare continuous off-line SEC/MALDI TOFMS with on-line SEC/ESI TOFMS (*28*). They found that the electrospray technique is more effective at characterizing low-*M* oligomers and the MALDI technique is more effective at characterizing high-*M* oligomers. Inductively coupled plasma MS (ICPMS) is a quite popular detection method for the SEC quantitation of metals across the elution profile of polymers. Sadi et al. listed several precautions that must be taken when coupling SEC to ICPMS (*29*). The use of organic solvents should be kept to a minimum because they affect the stability of the plasma. The ionic strength of the mobile phase buffers must be adjusted carefully because they can help limit non-SEC behavior, but they may also denature the organometallic complexes of interest. In addition, the salt content of the mobile phase should be kept to a minimum to avoid clogging the nebulizer and to reduce wear on the sampler and skimmer cones.

Sample preparation for this technique is also tricky because the species of interest must be extracted from the sample matrix without altering the nature of these species. Gardner et al. used SEC/ICPMS along with a UV detector to study metals in natural waters (*30*). Hall et al. used SEC/ICPMS to fractionate lead-bound ligands in human amniotic fluid and to detect and quantitate lead (*31*). In the realm of glycopolymers, Szpunar's group has used SEC/ICPMS along with DRI. The concentration-sensitive detector characterized the elution profiles of water-soluble and enzymatically digested polysaccharides, and the MS detector provided the distribution patterns of select metals in high- and low-*M* fractions of apple and carrot samples (*32*).

Other MS methods have also been coupled on-line to SEC, including chemical reaction interface MS to analyze nucleic acids, proteins, and other biopolymers (*33*), as well as atmospheric-pressure chemical ionization MS to determine pesticide binding by humic substances (*34*).

Spectroscopic detectors

The IR detector can act as either a chemical or a physical detector, and it can be used in on-line or continuous off-line modes. In off-line use, the same commercially available hardware used for SEC/MALDI can often be used for SEC/FTIR. The applications of FTIR as a physical detector have thus far been on-line and limited to characterizing the short-chain branching content of polyolefins. Markovich et al. used SEC/FTIR to measure the methyl group content per 1000 carbons, as a function of *M*, of ethylene-based polyolefin copolymers (*35*). Figure 6 shows a more recent example by DesLauriers, who used on-line SEC/FTIR and chemometrics to quantitate the ethyl and/or butyl content of ethylene 1-olefin copolymers as a function of *M* and related the results to trends resulting from catalysis and process changes (*36*).

Cotts and Ouano used IR as a chemical detector to study poly(vinyl butyral), which is actually a random terpolymer and is

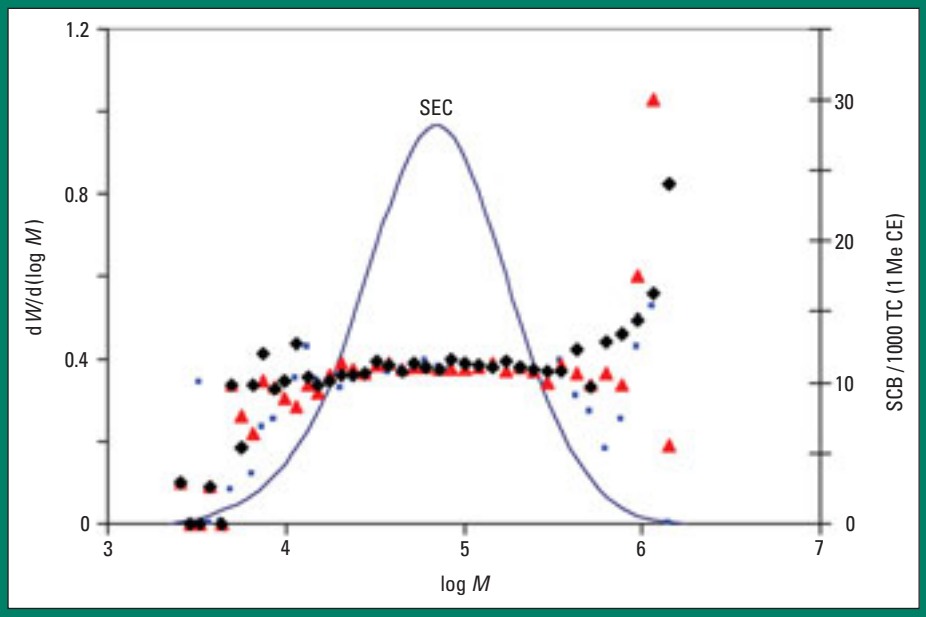

FIGURE 6. Short-chain branching in polyolefins by SEC/FTIR.

Distribution of the number of short-chain branches (SCB) with one methyl chain-end (1 Me CE) per 1000 total carbons (TC) across the MMD of an ethylene 1-olefin copolymer. Each type of symbol represents one run through the column. (Adapted from Ref. 36; figure provided courtesy of Paul DesLauriers, Chevron Phillips.)

more accurately referred to as poly(vinyl butyral-*co*-vinyl alcohol-*co*-vinyl acetate) (*12*, *37*). By monitoring the OH stretch of the hydroxyl group and the butyral ring vibration, they found the vinyl alcohol content of the polymer to be independent of *M*. Most applications of FTIR as a chemical detector are continuous and off-line. The SEC eluent is directed to a heated nozzle for evaporation of the solvent and deposition of the analyte onto a rotating germanium disk; spectra are obtained from any location on the disk (*38*, *39*).

To date, all SEC/NMR experiments have been performed in continuous (not stop-flow) mode, and all reports have dealt with SEC/^{1}H-NMR (*40*). The use of NMR as a physical detector appears to be thus far restricted to measurement of the tacticity distribution in mixtures of isotactic and syndiotactic PMMA (*41*). As a chemical detector for SEC, on-line coupling of NMR has been used to determine the MMD of uniformly isotactic PMMA (*42*) and to study the chemical heterogeneity of synthetic copolymers (i.e., the change in chemical composition as a function of molar mass; *43*). Neiss and Cheng reported recently on the SEC/NMR analysis of alginates, in which the microstructure of these plant polysaccharides was determined in combination with Markov statistical models, off-line ^{13}C-NMR, and enzymology (*44*).

In addition to its widespread use as a concentration-sensitive detector, UV–vis has also been used to determine the chemical heterogeneity of copolymers, for example, in the study of poly(styrene-*co*-methyl methacrylate)s by SEC/DRI/UV/MALS (*45*). The DRI served as a concentration-sensitive detector, and the UV detector monitored λ = 262 nm, where styrene presents a strong absorption band but methyl methacrylate does not absorb. The weight fraction of styrene was quantitated across the MMD of the copolymers.

Fluorescence spectroscopy is growing in popularity as a detection method for SEC. Fauser and colleagues separated airborne organic molecules from bitumen by SEC, identifying these particles by on-line fluorescence detection (*46*). In studying dissolved organic matter from Baltic Sea water, Lepane isolated the hydrophobic and hydrophilic fractions by adsorption chromatography and then characterized them by SEC/fluorescence (*47*). Moon and co-workers monitored the coupling of fluorescence-labeled anhydride-functional polystyrene and PMMA in dilute polymer blends with SEC/fluorescence (*48*). Maliakal et al. used the same method to measure polymer–polymer chain-end reaction rate constants (*49*).

Edwards et al. attempted to use SEC/FT-Raman MS with a low-volume flow cell to characterize the microstructural variation in polybutadiene polymers as a function of elution volume (*50*). As an on-line detector, the Raman spectrometer lacked the necessary sensitivity to provide quantitative information for the particular analytes being examined because of its low sensitivity at the different excitation wavelengths. This setup is still promising, however, provided the proper experimental conditions can be found for the analyte solutions so that they exhibit a high scattering intensity relative to the solvent or mobile phase.

The use of conductivity detection in SEC has been rather sparse, despite its great potential for the analysis of polyelectrolytes. Rinaudo et al. used SEC/DRI/VISC/conductivity to measure the charge distribution, which was superimposed upon the MMD, for a series of sodium carboxymethylcelluloses (*51*).

Conclusions

For the purposes of determining both fundamental and end-use properties of macromolecules, multidetector SEC has come of age (*1*). The current focus is thus on obtaining the proper combination of detectors to characterize the physicochemical properties of interest. Physically, SEC/DRI/MALS/VISC has been shown to be extremely powerful and can now be augmented by on-line QELS. The combination of chemical detectors has also become impressive with the recent report of characterizing polymer additives using SEC/UV/^{1}H-NMR/ESI-MS/FTIR—the first three detectors were on-line, and the FTIR operated in continuous off-line mode (*52*). The constant conversion of analytical techniques into SEC detection methods provides a growing choice of parameters that can be measured.

André M. Striegel is an assistant professor at Florida State University. His research interests include the study of natural and synthetic polymers—in particular, applying multidetector SEC and related techniques to determine structure–property relationships of macromolecules and elucidating fundamental aspects of separation science. Address correspondence about this article to Striegel at Department of Chemistry & Biochemistry, Florida State University, Tallahassee, FL 32306-4390 (striegel@chem.fsu.edu).

References

(1) Striegel, A. M., Ed. *Multiple Detection in Size-Exclusion Chromatography*; ACS Symposium Series 893; American Chemical Society: Washington, DC, 2005.

(2) Yau, W. W.; Kirkland, J. J.; Bly, D. D. *Modern Size-Exclusion Liquid Chromatography*; Wiley: New York, 1979.

(3) Wu, C.-S., Ed. *Handbook of Size-Exclusion Chromatography and Related Techniques*; Marcel Dekker: New York, 2003.

(4) Teraoka, I. *Polymer Solutions: An Introduction to Physical Properties*; Wiley: New York, 2002; pp 108–135 for SLS; pp 167–200 for QELS; pp 209–220 for VISC.

(5) Wyatt, P. J. *Anal. Chim. Acta* **1993**, *272*, 1–40.

(6) Reed, W. F. In *Multiple Detection in Size-Exclusion Chromatography*; Striegel, A. M., Ed.; ACS Symposium Series 893; American Chemical Society: Washington, DC, 2005; pp 13–51.

(7) Striegel, A. M.; Timpa, J. D. In *Strategies in Size Exclusion Chromatography*; Potschka, M.; Dubin, P. L., Eds.; ACS Symposium Series 635; American Chemical Society: Washington, DC, 1996; pp 366–378.

(8) Striegel, A. M. In *Encyclopedia of Chromatography*, 2nd ed.; Cazes, J., Ed.; Marcel Dekker: New York, 2005; pp 1006–1010.

(9) Grcev, S.; Schoenmakers, P.; Iedema, P. *Polymer* **2004**, *45*, 39–48.

(10) Zimm, B. H.; Stockmayer, W. H. *J. Chem. Phys.* **1949**, *17*, 1301–1314.

(11) Burchard, W. *Adv. Polym. Sci.* **1999**, *143*, 113–194.

(12) Striegel, A. M. *Polym. Int.* **2004**, *53*, 1806–1812.

(13) Striegel, A. M. In *Multiple Detection in Size-Exclusion Chromatography*; Striegel, A. M., Ed.; ACS Symposium Series 893; American Chemical Society: Washington, DC, 2005; pp 76–93.

(14) Haney, M. *Lab. Equip.* **2003**, *39*, S14–S16.

(15) Witten, T. A. *Rev. Mod. Phys.* **1998**, *70*, 1531–1544.

(16) Berne, B. J.; Pecora, R. *Dynamic Light Scattering*; Dover Publications: Mineola, NY, 1976.

(17) Liu, Y.; et al. *Polymer* **2003**, *44*, 7209–7220.

(18) Cotts, P. M. In *Multiple Detection in Size-Exclusion Chromatography*; Striegel, A. M., Ed.; ACS Symposium Series 893; American Chemical Society: Washington, DC, 2005; pp 52–75.

(19) Striegel, A. M.; Alward, D. B. *J. Liq. Chromatogr. Relat. Technol.* **2002**, *25*, 2003–2022; erratum in *J. Liq. Chromatogr. Relat. Technol.* **2003**, *26*, 157–158.

(20) Striegel, A. M.; Krejsa, M. R. *J. Polym. Sci., Part B: Polym. Phys.* **2000**, *38*, 3120–3135.

(21) Roovers, J. *Plast. Eng. (Star and Hyperbranched Polymers)*, **1999**, *53*, 285–341.

(22) Striegel, A. M. *J. Biochem. Biophys. Methods* **2003**, *56*, 117–139.

(23) Prokai, L. *Int. J. Polym. Anal. Charact.* **2001**, *6*, 379–391.

(24) Deery, M. J.; Stimson, E.; Chappell, C. G. *Rapid Commun. Mass Spectrom.* **2001**, *15*, 2273–2283.

(25) Fei, X.; Murray, K. K. *Anal. Chem.* **1996**, *68*, 3555–3560.

(26) Lou, X.; van Dongen, J. L. J. *J. Mass Spectrom.* **2000**, *35*, 1308–1312.

(27) Esser, E.; et al. *Polymer* **2000**, *41*, 4039–4046.

(28) Liu, X. M.; et al. *J. Am. Soc. Mass Spectrom.* **2003**, *14*, 195–202.

(29) Sadi, B. B. M.; Vonderheide, A. P.; Becker, J. S.; Caruso, J. A. In *Multiple Detection in Size-Exclusion Chromatography*; Striegel, A. M., Ed.; ACS Symposium Series 893; American Chemical Society: Washington, DC, 2005; pp 168–183.

(30) Gardner, W. S.; Landrum, P. F.; Yates, D. A. *Anal. Chem.* **1982**, *54*, 1196–1198.

(31) Hall, G. S.; Zhu, X.; Martin, E. G. *Anal. Commun.* **1999**, *36*, 93–95.

(32) Szpunar, J.; et al. *J. Anal. At. Spectrom.* **1999**, *14*, 639–644.

(33) Lecchi, P.; Abramson, F. P. In *Multiple Detection in Size-Exclusion Chromatography*; Striegel, A. M., Ed.; ACS Symposium Series 893; American Chemical Society: Washington, DC, 2005; pp 184–195.

(34) Klaus, U.; Pfeifer, T.; Spiteller, M. *Environ. Sci. Technol.* **2000**, *34*, 3514–3520.

(35) Markovich, R. P.; Hazlitt, L. G.; Smith-Courtney, L. In *Chromatography of Polymers*; Provder, T., Ed.; ACS Symposium Series 521; American Chemical Society: Washington, DC, 1993; pp 270–276.

(36) DesLauriers, P. J. In *Multiple Detection in Size-Exclusion Chromatography*; Striegel, A. M., Ed.; ACS Symposium Series 893; American Chemical Society: Washington, DC, 2005; pp 210–229.

(37) Cotts, P. M.; Ouano, A. C. In *Microdomains in Polymer Solutions*; Dubin, P., Ed.; Plenum Publishing: New York, 1985; pp 101–119.

(38) Willis, J. N.; Dwyer, J. L.; Liu, M. X. *Int. J. Polym. Anal. Charact.* **1997**, *4*, 21–29.

(39) Karami, A.; Balke, S. T.; Schunk, T. C. *J. Chromatogr., A* **2001**, *911*, 27–37.

(40) Albert, K.; et al. *J. High Resolut. Chromatogr.* **1999**, *22*, 135–143.

(41) Ute, K.; et al. *Macromol. Chem. Phys.* **2001**, *202*, 3081–3086.

(42) Ute, K.; et al. *Polym. J.* **1998**, *30*, 439–443.

(43) Krämer, I.; et al. *Macromol. Chem. Phys.* **1999**, *200*, 1734–1744.

(44) Neiss, T. G.; Cheng, H. N. In *NMR Spectroscopy of Polymers in Solution and in the Solid State*; Cheng, H. N., English, A. D., Eds.; ACS Symposium Series 834; American Chemical Society: Washington, DC, 2003; pp 382–395.

(45) Medrano, R.; et al. *Phys. Chem. Chem. Phys.* **2003**, *5*, 151–157.

(46) Fauser, P.; et al. *Pet. Sci. Technol.* **2000**, *18*, 989–1007.

(47) Lepane, V. *Oil Shale* **2001**, *18*, 239–257.

(48) Moon, B.; Hoye, T. R.; Macosko, C. W. *J. Polym. Sci., Part A: Polym. Chem.* **2000**, *38*, 2177–2185.

(49) Maliakal, A.; O'Shaughnessy, B.; Turro, N. J. In *Multiple Detection in Size-Exclusion Chromatography*; Striegel, A. M., Ed.; ACS Symposium Series 893; American Chemical Society: Washington, DC, 2005; pp 114–129.

(50) Edwards, H. G. M.; Johnson, A. F.; Lewis, I. R. *J. Raman Spectrosc.* **1993**, *24*, 435–441.

(51) Rinaudo, M.; Danhelka, J.; Milas, M. *Carbohydr. Polym.* **1993**, *21*, 1–5.

(52) Ludlow, M.; et al. *J. Chromatogr., A* **1999**, *857*, 89–96.